Wideband 400-element electronically reconfigurable transmitarray in X band

Antonio Clemente, Laurent Dussopt, Ronan Sauleau, Potier Patrick, Philippe Pouliguen

Wideband 400-element Electronically Reconfigurable Transmitarray in X Band

Antonio Clemente, *Student Member, IEEE,* Laurent Dussopt, *Senior Member, IEEE,* Ronan Sauleau, *Senior Member, IEEE,* Patrick Potier, and Philippe Pouliguen

***Abstract*— A fully electronically reconfigurable 400-element transmitarray is studied numerically and experimentally in X-band. The array operates in linear polarization and consists of 20×20 unit-cells. A 1-bit phase resolution has been selected for the unit-cell in order to reduce the complexity of the biasing network and steering logic, the insertion loss and the overall cost of the antenna system. The unit-cell stack-up is simple and is made of four metal layers: active side, biasing lines, ground plane and passive side. Two p-i-n diodes are integrated on the active side of each cell in order to control its transmission phase. The active array contains 800 diodes in total. It demonstrates experimentally pencil beam scanning over a 140×80-degree window over a 15.8% fractional bandwidth, with a maximum gain of 22.7 dBi at broadside. We also show that the same antenna array can be used for beam shaping applications (flat-top beam). The experimental results presented between 8 and 12 GHz are in good agreement with the theoretical performance calculated using full-wave electromagnetic simulations and an in-house CAD tool based on analytical modeling.**

***Index Terms*— Reconfigurable transmitarray antenna, array lens, discrete lens, 2D beam scanning, beam shaping, active microstrip array.**

I. Introduction

HIGH gain electronically reconfigurable antenna arrays are requested in many emerging applications at microwaves and millimeter waves. Thanks to their spatial feeding technique, reflectarray antennas [1] and transmitarrays are very attractive compared to traditional phased arrays which suffer from large insertion loss in their beam forming network. Transmitarrays have excellent capabilities for real-time beam steering and beam synthesis, and could be employed in a number of military and civil telecommunication and radar systems. Like reflectarrays, transmitarrays can also be used as focal lenses for large reflector antennas [2] in order to compensate for surface errors [3], produce contoured beams [4], or steer the beam in a limited angular range [5],[6].

A generic transmitarray structure is represented in Fig. 1a. One (or more [7]) focal source illuminates a first array of printed elements operating in receiving mode (*Rx* array); this array is connected, through a phase-shifter network, to a second array of printed elements operating in transmission mode (*Tx* array). In this way, by tuning the transmission phase of each unit-cell, the spherical wave radiated by the focal source and illuminating the *Rx* array can be transformed into a nearly plane wave radiating in the desired direction. Printed Circuit Board (PCB) technologies are often preferred to build the antenna stack-up, and various approaches using via holes [8],[9], delay lines [10],[11] or coupling slots [12] have been implemented to connect the *Rx* and *Tx* printed arrays. The transmission phase can be controlled using phase shifters [13] or by tuning the length of the delay line [10],[11], the size of the slot [14] or by rotating the *Rx* and *Tx* patch antennas with respect to each other [8],[9]. MEMS switches [15],[16], varactor diodes [14],[17]-[19], integrated ferroelectric varactors [20] or p-i-n diodes [21] have been used for the design of reconfigurable unit-cells.

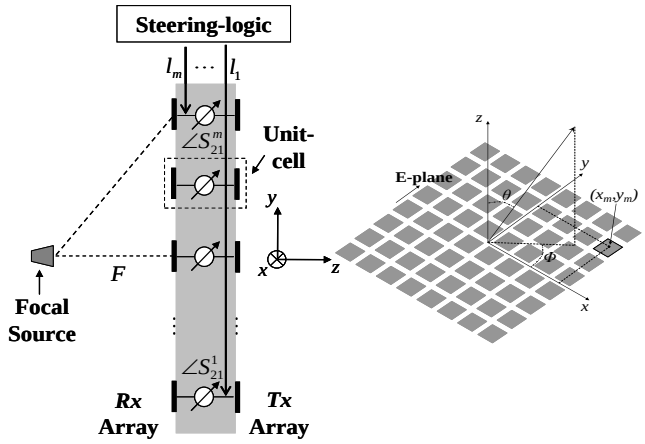

(a) (b)

Fig. 1. (a) Geometry of the transmitarray antenna with its steering logic (one bias / control line per unit-cell), and (b) definition of the coordinate system.

In our previous works in X band [21],[22], we demonstrated a 1-bit reconfigurable unit-cell based on p-i-n diodes with excellent experimental performance in terms of insertion losses (1.87 dB) and 3-dB bandwidth (14.7%). Its design rules, electrical equivalent circuit and 1-dB compression point have been studied in detail in [21].

This unit-cell is used here as a building block for the design of a 20×20-element fully reconfigurable transmitarray. The realized prototype exhibits a wide 3-dB bandwidth and an excellent 2-D beam-steering capability. To the authors' best knowledge, this prototype is one of the largest reconfigurable

Manuscript received November 5, 2012; revised May 10, 2013.

A. Clemente and L. Dussopt are with CEA-LETI, Minatec Campus, F38054 Grenoble, France (e-mail: antonio.clemente.ca@gmail.com, laurent.dussopt@cea.fr).

R. Sauleau is with the Institute of Electronics and Telecommunications of Rennes (IETR), UMR CNRS 6164, University of Rennes 1, F35042, Rennes, France (e-mail: ronan.sauleau@univ-rennes1.fr).

P. Potier is with the Direction Générale de l'Armement (DGA), F35174, Bruz cedex, France (e-mail: patrick.potier@dga.defense.gouv.fr).

P. Pouliguen is with the Direction Générale de l'Armement (DGA), Strategy Directorate, Office for Advanced Research and Innovation, F92221 Bagneux cedex, France (e-mail: philippe.pouliguen@dga.defense.gouv.fr).

transmitarray presented in the open literature, and its radiation efficiency is among the highest reported so far (52.9%).

This paper is organized as follows. The antenna architecture (Section II.A) and its design (Section II.C) and fabrication (Section II.D) are described in Section II. The main characteristics of the unit-cell [21] are also summarized in Section II.B. Then, the antenna performance is given in Section III for beam scanning and beam shaping. Finally conclusions are drawn in Section IV.

II. Transmitarray Architecture, Design and Fabrication

A. Description of the antenna system

The proposed transmitarray comprises 20×20 unit-cells distributed over a regular square grid and consists in practice of 2×2 identical 100-element sub-arrays with their own steering logic (Fig. 2a). The layout (active side and bias lines) of one sub-array is represented in Fig. 2b, and the unit-cell (geometry, performance) will be described in Section II.B. The inter-element spacing is 15 mm ($\lambda_0/2$ at 10 GHz) in *x*- and *y*-directions, which prevents from the appearance of grating lobes over the array bandwidth (9–10.6 GHz) and scanning range (±70° from broadside).

Here, each unit-cell is controlled individually using a single bias line per cell. Therefore, each antenna sub-array contains 100 independent bias lines (1 line per unit-cell), as illustrated in Fig. 2b. Therefore, depending on its location within a sub-array, each unit-cell may include from one to ten bias lines passing by in the vicinity of the active patch. We will show in Section II.B that these lines do not have any substantial effect on the RF performances, so that more bias lines may be accommodated for the design of larger arrays.

In contrast to many other designs of reconfigurable unit-cells for reflectarrays [23]-[27] and transmitarrays [14],[16]-[19], the phase resolution of the proposed unit-cell in transmission is only 1-bit here (180°). Such a choice allows reducing the complexity and insertion loss of the unit-cell [21] as well as the total number of active components within the array (only two diodes / unit-cell). This facilitates the routing of the bias / control lines within the antenna layout, as shown in Fig. 2b.

An analytical preliminary analysis was performed to study the impact of the phase quantization on the pointing direction when beam steering is synthesized from a simple linear phase distribution as detailed in Section II-C. A maximum error of +0.5°/-1.2° is obtained between the desired and effective scan angles for a 1-bit phase quantization and for a scan angle up to 60° (Fig. 3b). This is to be compared with a maximum error of 0.8° for the same array without phase quantization (Fig. 3a); in this latter case, the error is due to the $cos\theta$ radiation pattern of the unit-cell (no error would occur for omnidirectional unit-cells). Therefore, the impact of the phase quantization can be considered acceptable as it is significantly smaller than the 3-dB beamwidth (~6°).

B. Unit-cell: geometry and performance

The transmitarray unit-cell (Fig. 4a), presented in our previous papers [21],[22], is fabricated on two substrates (Roger RO4003, ε_r = 3.55 at 10 GHz, tanδ = 0.0027, and *h* =

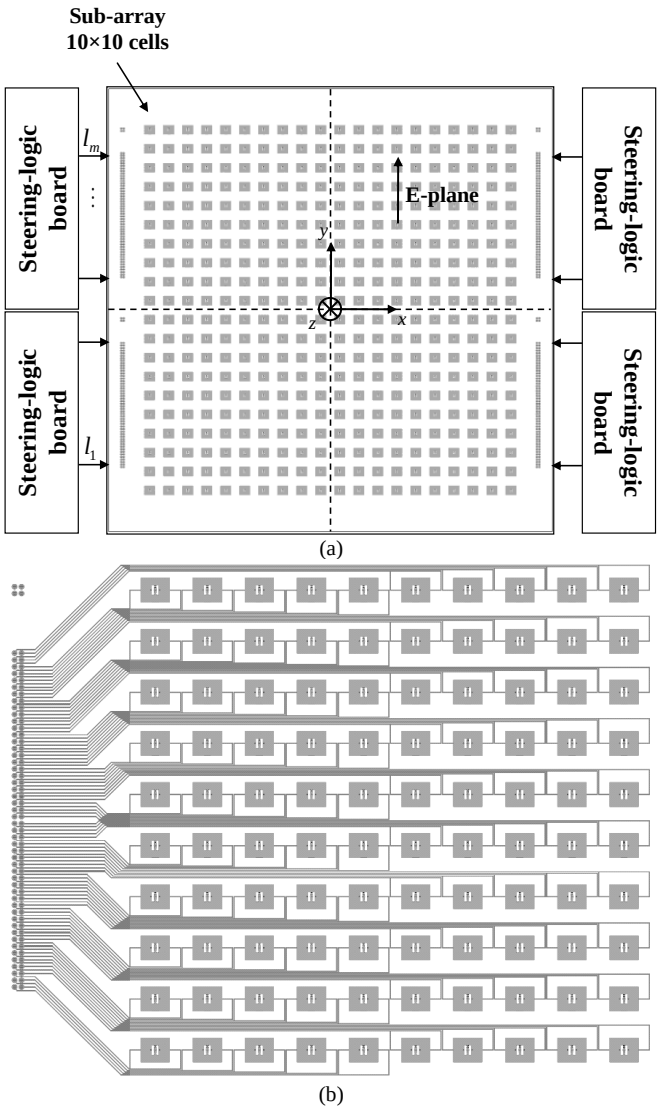

Fig. 2. (a) Antenna panel with its four steering logic units (1 steering logic per 10×10-element sub-array). (b) Layout of a 10×10-element sub-array and its biasing network. The unit-cell is described in Section II.B.

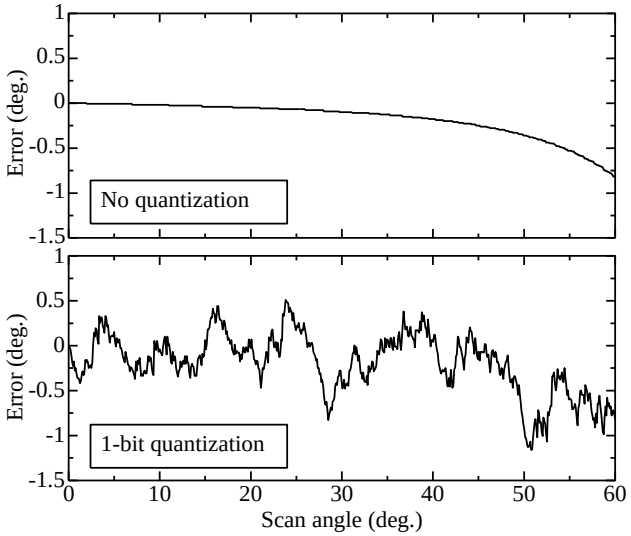

Fig. 3. Error between the desired and effective scan angle for two cases: no phase quantization, 1-bit phase quantization.

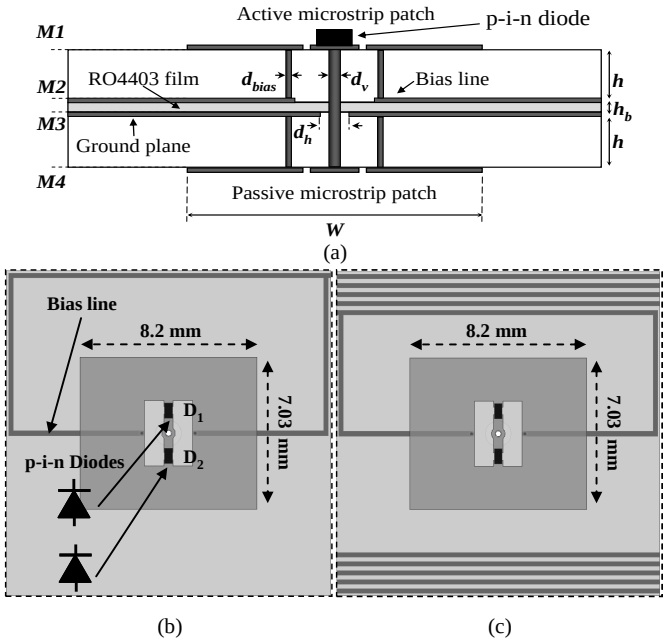

Fig. 4. 1-bit electronically reconfigurable unit-cell. (a) Cross-section view (d_h = 600 µm) [21]. Top view of a unit-cell with 1 bias line (b) and (c) 10 bias lines.

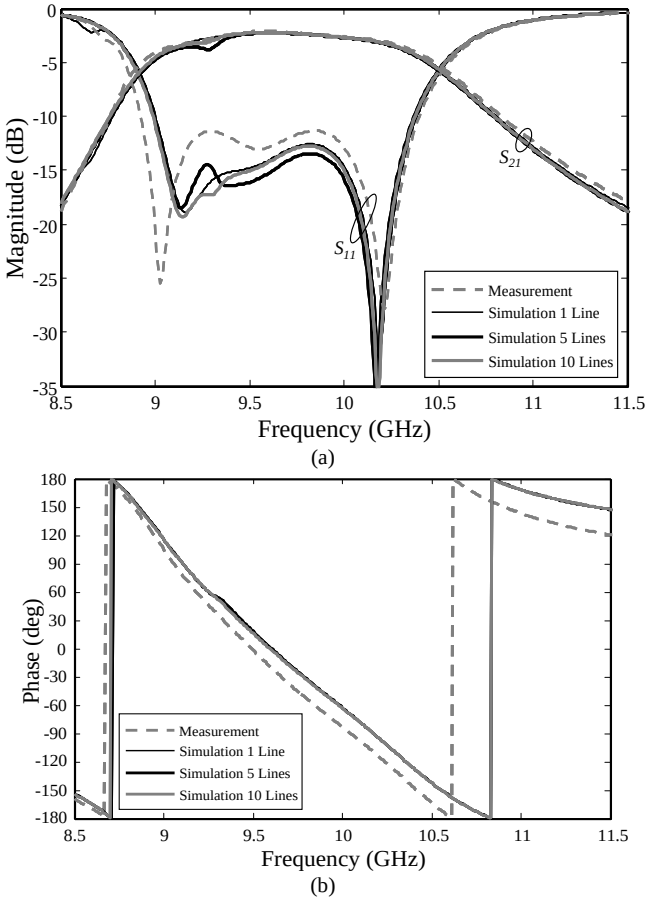

Fig. 5. Measured (unit-cell with 1-bias line) and simulated (1, 5, or 10 bias lines) (a) amplitude of the reflection and transmission coefficients and (b) transmission phase of the 1-bit reconfigurable unit-cell. The unit-cell is in the 0° phase state.

1.524 mm) bonded with a thin (h_b = 100 µm) RO4403 film. The resulting dielectric stack-up contains only four 18 µm-thick metal layers (M1 to M4). The passive and active patch antennas are rectangular (7.03×8.2 mm²); they are printed on both external faces of the assembly (M4 and M1, respectively) and are connected by a metallized via hole (d_v = 360 µm in diameter). The ground plane is printed on one of the two inner layers (M2), and the bias lines on the second inner metal layer (M3).

The passive patch antenna is loaded by a U-slot and is connected to the ground plane for biasing purposes through two vertical via holes (d_{bias} = 150 µm) placed on the zero-voltage median-line of the patch. The active patch antenna (Fig. 4b) is loaded by an O-slot and is connected to the bias line by two vertical via holes (d_{bias} = 150 µm). Two p-i-n diodes (0.68×0.36×0.19 mm^3, [28]) are integrated in the active patch as shown in Fig. 4b. This configuration allows polarizing both diodes in opposite states using a single bias line with a positive or negative current, and leads to a 1-bit (0°/180°) phase shift as demonstrated in [21]. The frequency response of this reconfigurable cell has been computed using Ansys-HFSS with periodic boundary conditions and Floquet ports.

The unit-cell prototypes have been characterized using an *ad-hoc* waveguide experimental setup [21]. The measured amplitude of the transmission (S_{21}) and reflection (S_{11}) coefficients are presented in Fig. 5a for the 0°-phase state and a 10-mA bias current (D_1 *on*, D_2 *off*). This figure shows that the cell exhibits 2.1 dB of insertion loss at 9.6 GHz and a 14.9 % 3-dB fractional bandwidth. Due to the geometrical symmetry of the cell, similar results (not shown) are obtained in the 180°-phase state (D_2 *on*, D_1 *off*). The measured differential phase shift exhibits a maximum phase deviation of 13° around 180° between 8.8 GHz and 11.5 GHz (Fig. 9 in [21]).

In order to study the impact of the bias lines on the cell frequency response, several simulations have been performed by considering 1, 5 or 10 bias lines per cell (Figs. 4b and 4c). The scattering parameters (solid lines in Fig. 5) are almost the same in all cases, demonstrating thereby that the DC bias lines do not impact the RF performance. This is due to the fact that the bias lines are very narrow (210 µm), close to the ground

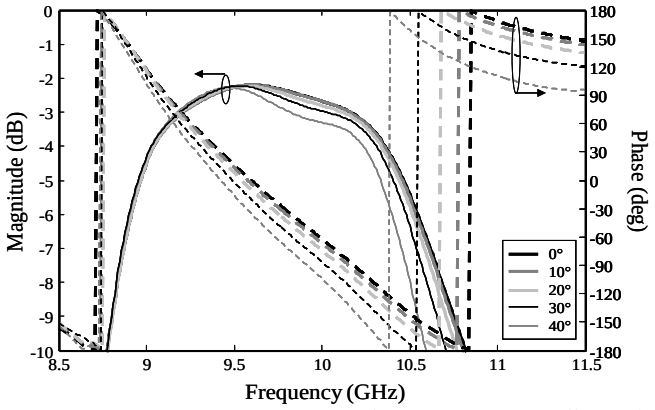

Fig. 6. Simulated magnitude and phase of the transmission coefficient for various incidence angles. The unit-cell is in the 0° phase state.

plane (h_b = 100 µm) and perpendicular to the electric field polarization of the active patch.

Finally, the S_{21} parameter has been computed for several incidence angles up to 40°. The results are given in Table I and Fig. 6, showing small variations in magnitude (-2.15 to -2.38 dB) and phase (0–37.2°) at the center frequency.

TABLE I

TRANSMISSION COEFFICIENT OF THE UNIT-CELL AT 9.6 GHZ FOR SEVERAL INCIDENCE ANGLES (CELL IN THE 0°-PHASE STATE).

Incidence angle	0°	10°	20°	30°	40°
$\lvert S_{21}\rvert$ (dB)	-2.15	-2.15	-2.27	-2.27	-2.38
$ph(S_{21})$	0°	-3.32°	-9.64°	-20.3°	-37.2°

C. Design of the transmitarray

The relative phase $\varphi_m^{tr}(x_m, y_m)$ of the electromagnetic field radiated by unit-cell *m* (Fig. 1b) can be written as

$$\varphi_m^{tr}(x_m, y_m) = \varphi_{FS}(\theta_m, \phi_m) - k_0 r_m + \varphi_m^{inc}(\theta_{FS}, \phi_{FS}) + ph(S_{21}^m), \quad (1)$$

where $\varphi_{FS}(\theta_m, \phi_m)$ is the phase radiated by the focal source in the direction (θ_m, ϕ_m) of unit-cell *m*, k_0 is the wave number in vacuum at the center frequency f_0, $r_m = \sqrt{F^2 + x_m^2 + y_m^2}$ is the distance between the phase centers of the focal source and the unit-cell *m*, *F* is the focal distance, (x_m, y_m) are the coordinates of unit-cell *m*, $\varphi_m^{inc}(\theta_{FS}, \phi_{FS})$ is the phase of the radiation pattern of unit-cell *m* in the incident direction (θ_{FS}, ϕ_{FS}) from the focal source and $ph(S_{21}^m)$ is the phase shift introduced by unit-cell *m* (Fig. 1a).

On the other hand, the main beam of a planar phased array can be steered in a direction (θ_0, ϕ_0) using a simple linear phase distribution across the array aperture, as given by

$$\varphi_m(x_m, y_m) = -k_0 \sin\theta_0 \cos\phi_0 x_m - k_0 \sin\theta_0 \sin\phi_0 y_m, \quad (2)$$

By equating Eqns. (1) and (2), the required phase shift for each unit-cell is derived

$$ph(S_{21}^m) = k_0(r_m - \sin\theta_0 \cos\phi_0 x_m - \sin\theta_0 \sin\phi_0 y_m) - \varphi_m^{inc}(\theta_{FS}, \phi_{FS}) - \varphi_{FS}(\theta_m, \phi_m). \quad (3)$$

Eqn. (3) will be used in Sections III.A and III.B to define the phase distribution over the *Tx* array and scan the antenna beam in 2D over a large angular window. Shaped radiation patterns can also be generated using more complex phase distributions computed from beam-synthesis techniques, e.g. [29]-[33]. An example of flat-top beam is discussed in Section III.C.

Ideally, a continuous 360° phase tuning range would be desired for each unit-cell. As this is not feasible with switching devices such as p-i-n diodes, a discrete phase quantization is used to approximate the ideal transmission phase values with a resolution determined by the number of available phase states.

The unit-cell described in Section II.B provides two phase states (0° or 180°), and the array layout is defined according to the quantization rule $Q\left(ph(S_{21}^m)\right)$ given by

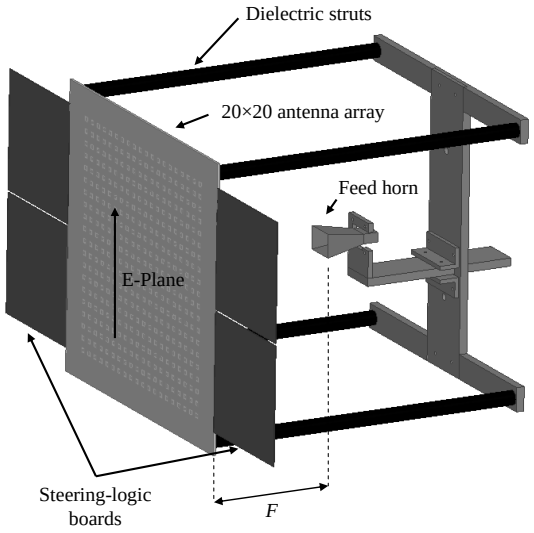

(a)

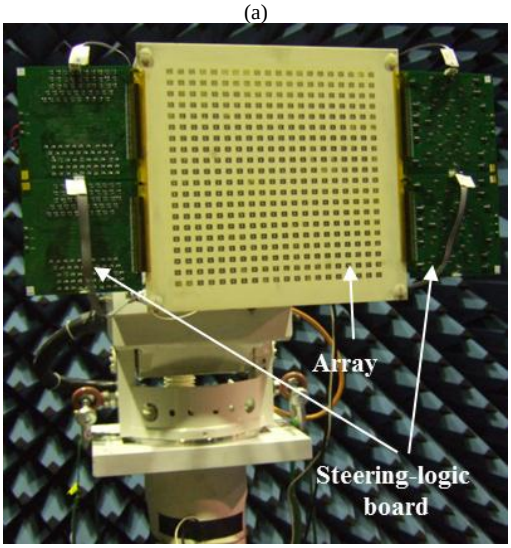

(b)

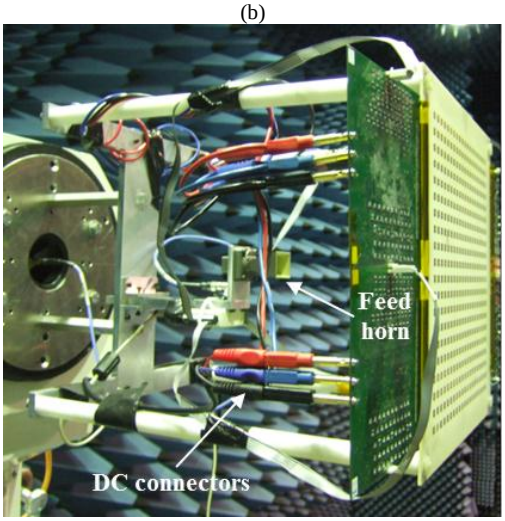

(c)

Fig. 7. Electronically reconfigurable transmitarray. (a) 3D schematic view. (b,c) Front and side view of the antenna prototype mounted in the anechoic chamber. The four steering logic boards are located on both sides of the antenna array in H-plane (they could have been placed perpendicular to the antenna panel to reduce the antenna footprint).

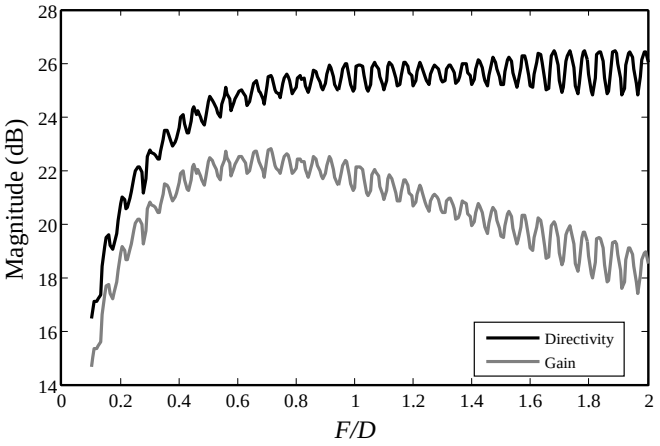

Fig. 8. Simulated directivity and gain as a function of the focal ratio F/D (f = 9.8 GHz).

$$Q\left(ph\left(S_{21}^{m}\right)\right)=\begin{cases}0^{\circ}\ \text{if}\ -\dfrac{\pi}{2}\le ph\left(S_{21}^{m}\right)<\dfrac{\pi}{2}\\ 180^{\circ}\ \text{otherwise}\end{cases} \quad (4)$$

For the 400-element array considered here, the 1-bit quantization leads to a reduction of the antenna directivity close to 4 dB, as compared to a 1.0/0.2 dB directivity loss for a 2/3-bits quantization, respectively. These figures are comparable to those reported in [34]-[36]. In practice, a higher phase resolution would require a more complex unit-cell geometry with a lot of active components and bias / control lines, which would increase significantly the insertion loss. Therefore, a trade-off must be often found between quantization loss and insertion loss. In this work, a 1-bit quantization has been selected to maximize the transmitarray efficiency [8],[21].

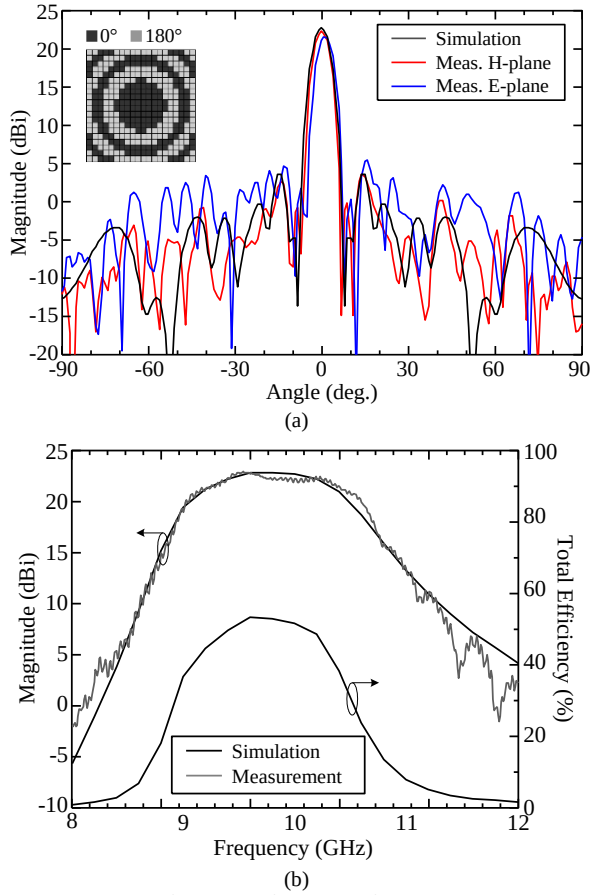

Fig. 9. Radiation performance of the reconfigurable transmitarray when radiating at broadside (F/D = 0.71). (a) Co-polarization components in E- and H-planes (f = 9.8 GHz) and unit-cell distribution (inset). (b) Antenna gain (measured and simulated) and total efficiency (simulated).

D. *Fabricated prototype and experimental setup*

The fabricated 400-element fully reconfigurable planar transmitarray is represented in Fig. 7. The radiating panel (360×360 mm²) has the same dielectric stack-up as in Fig. 4a and contains 800 p-i-n diodes (two diodes per unit-cell). It is surrounded by four steering-logic boards used to control the phase state of each unit-cell individually (Fig. 2a). The focal source is a linearly-polarized pyramidal standard gain horn antenna (SGH) with a 11.1-dBi gain at 10 GHz. A specific mechanical fixture with four dielectric struts in Delrin (diameter = 1 cm) holds the array and the focal source together and allows tuning the focal distance F in the range 160–330 mm ($0.44 < F/D < 0.92$).

Each steering-logic board (150×150 mm^2) drives a sub-array of 10×10 elements with a ±10 mA bias current per unit-cell. These boards are plugged along the edges of the transmitarray and are connected to the DC power supply and to the computer using a digital I/O USB module. The total power consumption is 12 mW (10 mA/1.2 V) for each unit-

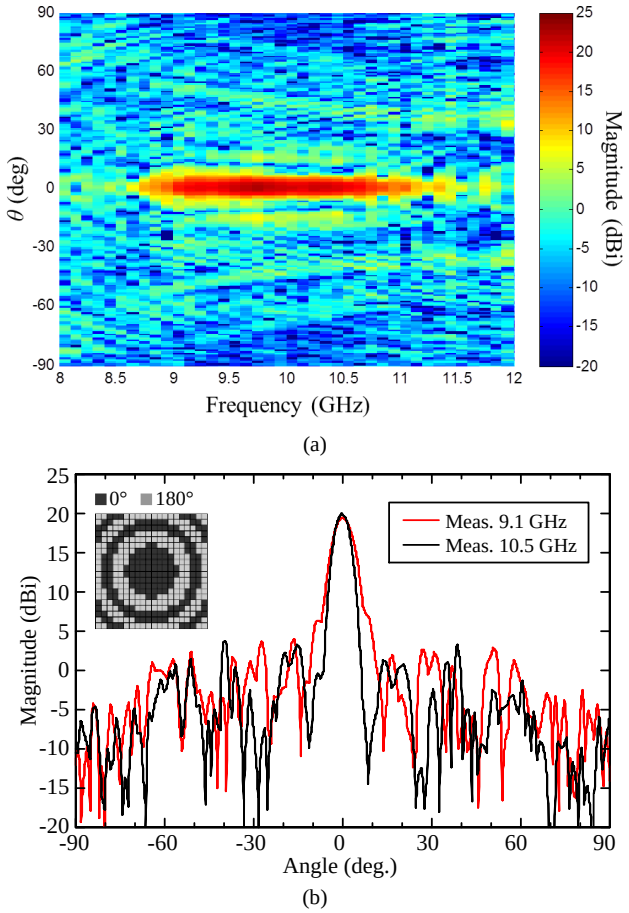

Fig. 10. (a) Gain measured as a function of frequency and elevation angle in H-plane (F/D = 0.71). (b) Measured gain radiation pattern in H-plane at 9.1 and 10.5 GHz.

cell and 4.8 W for the full array.

III. Beam Steering and Beam Shaping: Numerical and Experimental Results

The radiation characteristics of the transmitarray are computed using an in-house CAD tool based on an analytical model of the array and full-wave simulations of the focal source and the unit-cells [8]. They are measured in an anechoic chamber in the far field zone (the distance between the antenna under test and the transmitting antenna is 18 m).

A. Radiation at broadside

The antenna directivity and gain computed in the broadside direction (θ_0 =0°) are plotted in Fig. 8 at 9.8 GHz as a function of the F/D ratio (D = 300mm). The 0.5–1 dB ripples observed on these curves are due to the 1-bit phase quantization. For the same reason, the peak directivity reaches only 26.6 dBi for large focal distances, which corresponds to 4.4 dB of quantization loss compared to the maximum theoretical directivity (31 dBi) of a uniform $10\lambda_0 \times 10\lambda_0$ radiating aperture. This is in agreement with the 4-dB quantization loss estimated in Section II.B. The gain is maximum (22.8 dBi) for F/D = 0.71 (F = 214 mm). The corresponding directivity, spill-over loss and power efficiency are equal to 25.6 dBi, 1.34 dB, and 52.9%, respectively. The gain variation for an F/D ratio ranging from 0.4 to 1.1 is only ±0.5 dB.

The unit-cell distribution over the radiating aperture is represented in the inset of Fig. 9a for F/D = 0.71. It has been determined as explained in Section II.C. For this F/D ratio, the edge illumination with respect to the center is -8.21 dB and -7.42 dB in E-plane (ϕ_0 = 90°) and H-plane (ϕ_0 = 0°), respectively.

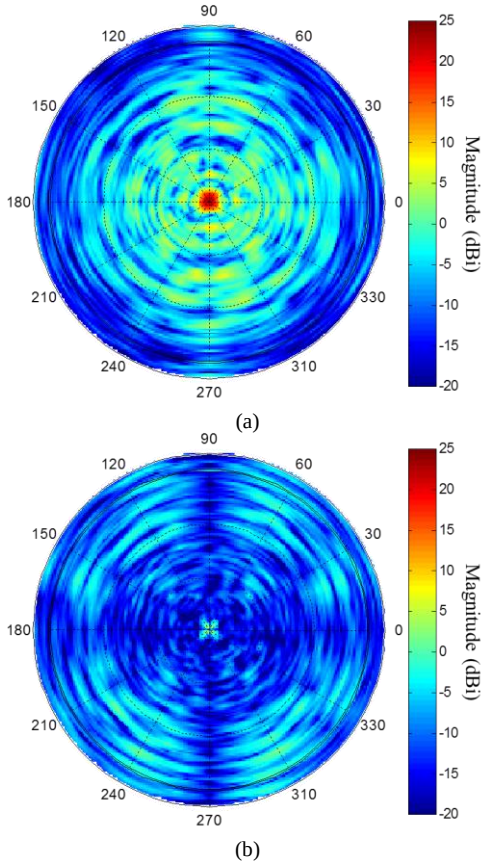

(a)

(b)

Fig. 11. Measured 2D radiation patterns at 9.8 GHz (F/D = 0.71). (a) Co-polarization component. (b) Cross-polarization component (Ludwig 3 [36],[37]).

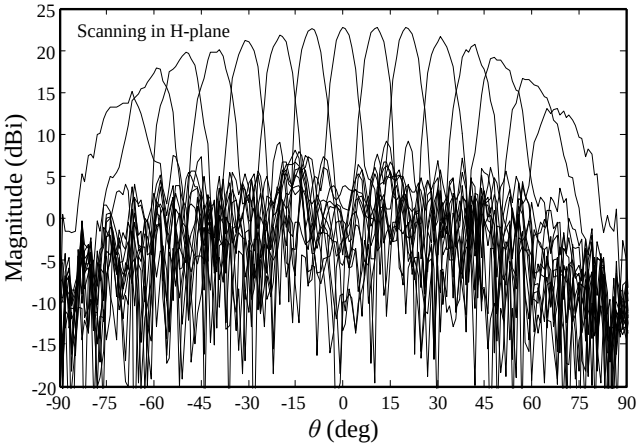

(a)

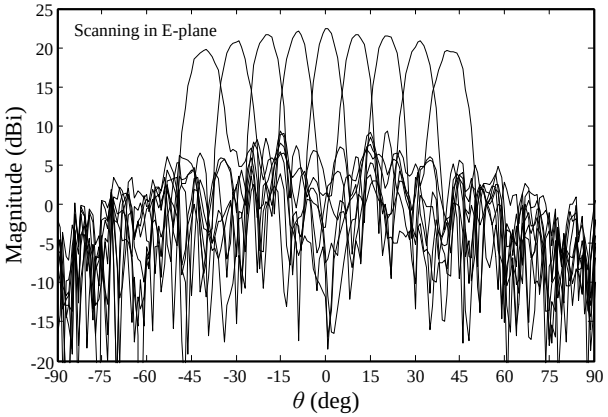

(b)

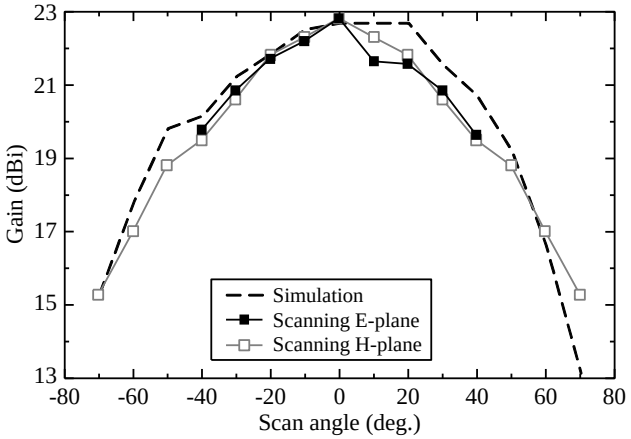

(c)

Fig. 12. (a,b) Measured radiation patterns for different scan angles in H-plane (a) and in E-plane (b). (c) Simulated and measured maximum gain as a function of the scan angle.

As the radiation patterns of the unit-cell are similar in both principal planes [21], the beam radiated by the transmitarray is almost identical in these two planes (Fig. 9a). A good agreement between simulations and measurements is obtained in the main beam and for the first side lobes. However, outside the ±30° angular sector, the observed discrepancies are more pronounced; this may be explained by edge diffraction effects and spill-over radiation that are not taken into account in the simulation. In particular, the gain of the focal source for elevation angles ranging between 30° to 90° is of the order or larger than the simulated side lobes of the array. This conclusion is further supported by the lower side lobes measured in H-plane where the steering-logic boards partially block this radiation (Fig. 7). At 9.8 GHz, the maximum values of the measured gain and computed directivity equal 22.7 dBi and 25.6 dBi, leading to an antenna efficiency of 52.9%.

The gain of the transmitarray has been measured over *X* band between 8 and 12 GHz (Fig. 9b). The measured 3-dB bandwidth reaches 1.58 GHz (9.02–10.6 GHz, 15.8% at 10 GHz); the ripples observed beyond 11 GHz are probably due to multiple reflections between the array and the focal source fixture since the unit-cells are not matched in this frequency range (Fig. 5a).

The gain measured in H-plane as a function of the elevation angle and frequency is plotted in Fig. 10a, while the radiation patterns measured at the bandwidth edges (9.1 and 10.5 GHz) are reported in Fig. 10b. As known from the array theory, the beamwidth decreases and the side lobes come closer to the main beam as frequency increases. The first side lobe remains below 8 dBi over X band. The experimental half-space radiation patterns confirm the good symmetry of the radiated beam (Fig. 11). In the two principal planes the side-lobe level (SLL) and cross-polarization component are 18.8 dB and 25-30 dB below the maximum, respectively.

B. Beam scanning

The beam steering capabilities of the transmitarray have been demonstrated through extensive measurement campaigns up to ±70° and ±40° in H-plane (Fig. 12a) and E-plane (Fig. 12b), respectively.

Due to the limited availability of the anechoic chamber at DGA-MI, Bruz, France, a 10° angular step has been selected between two consecutive main beam directions, and the measurement window has been restricted to ±40° in E-plane. In all cases, the phased state of each unit-cell is controlled by an external personal computer. In all configurations, the SLL remains at least 15 dB below the maximum, and the measured main beam directions well coincide with the target values.

Fig. 11c confirms that very similar radiation performance is measured when scanning the beam in E- and H-planes. The measured scan loss is lower than 3 dB over a ±39° window.

The measured co-polarization components are represented in Fig. 13 for four scan angles θ_0 (-10°, -20°, -30°, and -40°) in E- and H-planes. They are in quite good agreement with the numerical simulations, especially within the ±30° angular sector around the broadside direction where spill-over radiation from the focal source has no significant effect.

TABLE II
BEAM SCANNING PERFORMANCE IN H-PLANE.

	Dir (dBi)	**Gain (dBi)**		**3-dB beamwidth (deg)**		**SLL (dB)**	
Scan Angle θ_0	**Sim.**	**Sim.**	**Meas.**	**Sim.**	**Meas**	**Sim.**	**Meas.**
-70°	18.0	15.3	15.1	16.6	12.7	12.4	7.6
-60°	19.8	17.0	17.9	11.3	10.6	13.4	10.9
-50°	21.6	18.8	19.8	9.2	9.3	13.3	12.5
-40°	22.2	19.5	20.2	7.7	7.7	14.5	14.5
-30°	23.4	20.6	21.2	6.9	7.2	15.0	13.3
-20°	24.6	21.8	21.9	6.4	6.5	16.2	14.7
-10°	25.0	22.3	22.5	6.1	6.5	13.8	13.6
0°	25.6	22.8	22.7	6.0	6.1	19.2	18.8
10°	25.0	22.3	22.7	6.1	6.5	13.8	13.6
20°	24.6	21.8	22.7	6.4	6.7	16.2	15.3
30°	23.4	20.6	21.6	6.9	7.1	15.0	12.4
40°	22.2	19.5	20.8	7.7	7.2	14.5	14.7
50°	21.6	18.8	19.2	9.2	9.2	13.3	13.5
60°	19.8	17.0	16.6	11.3	10.3	13.4	9.9
70°	18.0	15.6	13.2	16.6	9.9	12.4	6.7

Outside this angular sector, spill-over radiation as well as spurious scattering on the array edges and steering logic boards degrade the radiation performances. Lower side lobes would be expected with a careful shielding of the spill-over radiation around the array. The main theoretical and experimental radiation performances of the transmitarray are summarized in Table II when scanning in H-plane. A gain and SLL variation of about 7.3 dB and 11.2 dB has been measured between the broadside and the 70°-steered patterns, respectively.

Figs. 14a and 14b represent the measured gain as a function of frequency and elevation angle for two scan angles in H-plane (20° and 60°, respectively). As expected, the effective scan angle decreases with frequency (beam squint) due to the constant-phase frequency response of the unit-cells. Finally, the beam steering capability of the transmitarray in the diagonal plane is demonstrated in Fig. 14c and Fig. 14d for an antenna beam pointing in the diagonal plane θ_0 = -40° and ϕ_0 = 135°. In this case, a maximum gain of 20.5 dBi is obtained, and the maximum cross-polarization level is 12.3 dB below the maximum in the main beam.

C. Beam shaping

Since each unit-cell of the transmitarray is controlled independently, any arbitrary phase distribution can be synthesized. In order to demonstrate the beamforming capabilities of this reconfigurable transmitarray, a flat-top beam pattern has been synthesized. The required phase distribution over the transmitarray aperture has been calculated using an *in-house* genetic algorithm optimization tool [39]-[41] coupled to our transmitarray simulation code [8]. The optimization was launched at 9.8 GHz for a fixed focal distance ($F = 0.71D$), and the mask power template is defined arbitrarily by a beamwidth of 80–90°, a ripple level less than 2 dB in the main beam, and a SLL below -20 dB. This mask is represented in dashed line in Fig. 15.

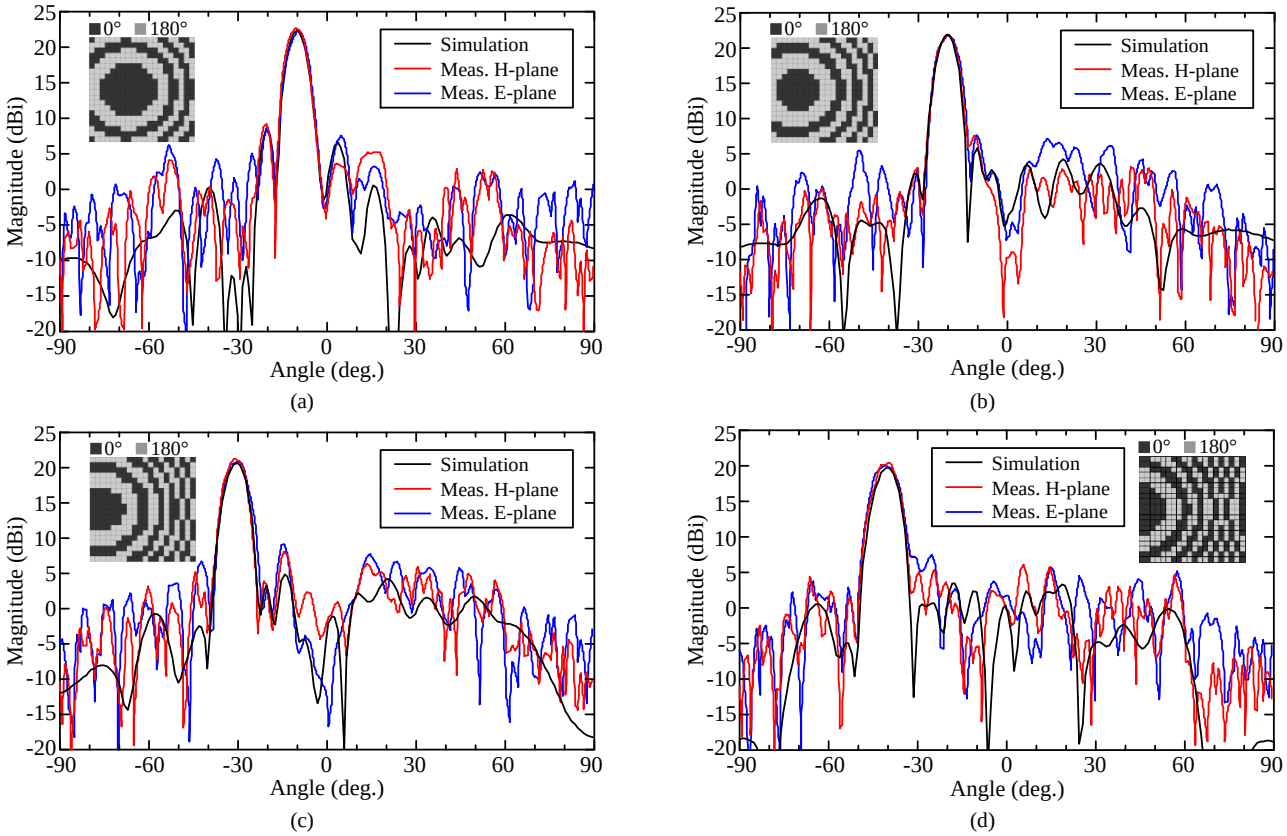

Fig. 13. Simulated and measured co-polarization components for several scan angles in H- and E-planes. (a) θ_0 = -10°. (b) θ_0 = -20°. (c) θ_0 = -30°. (d) θ_0 = -40°. f = 9.8 GHz. F/D = 0.71.

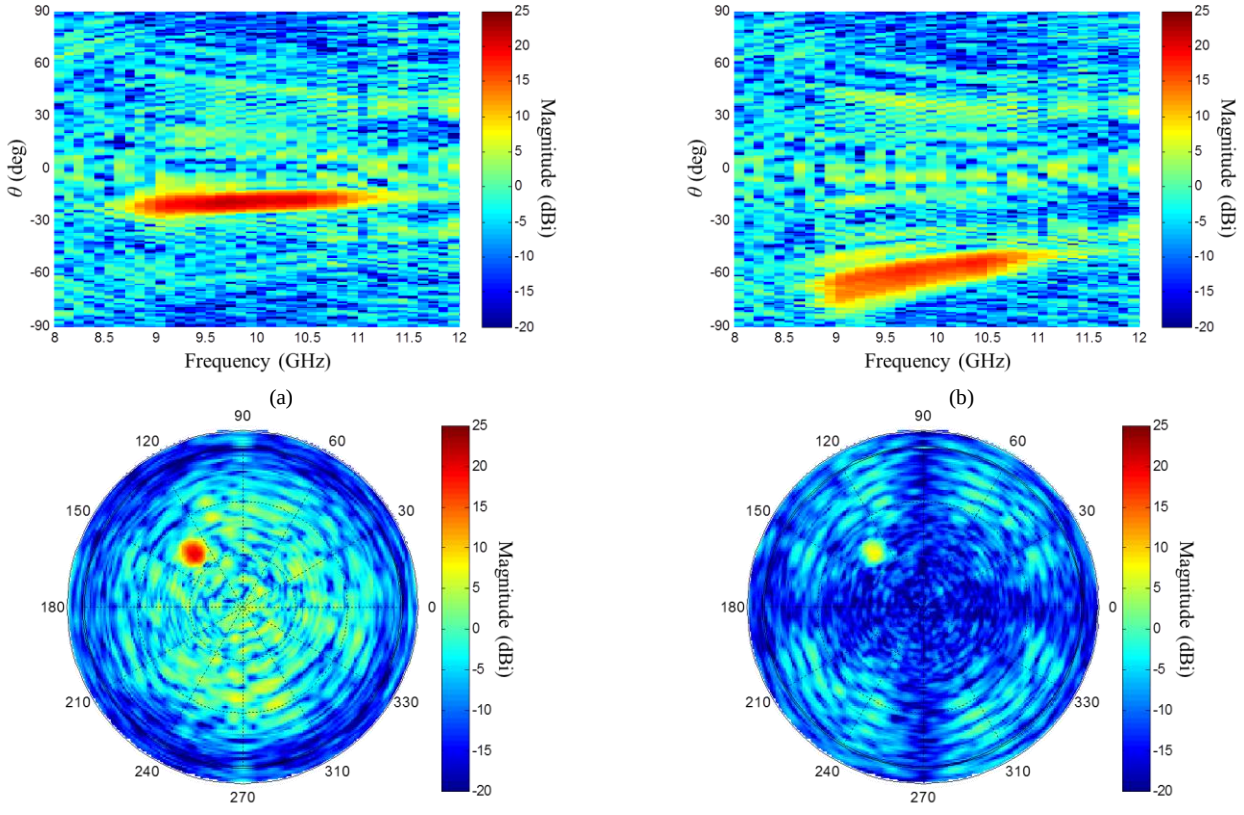

Fig. 14. (a,b) Measured gain as a function of frequency and elevation angle for two main beam directions in H-plane (ϕ_0 = 0°): (a) θ_0 = -20°, (b) θ_0 = -60°. (c) Co-polarization and (d) cross-polarization components for a scan angle of θ_0 = -40° (elevation) and ϕ_0 = 135° (azimuth) at 9.8 GHz. In all cases F/D = 0.71.

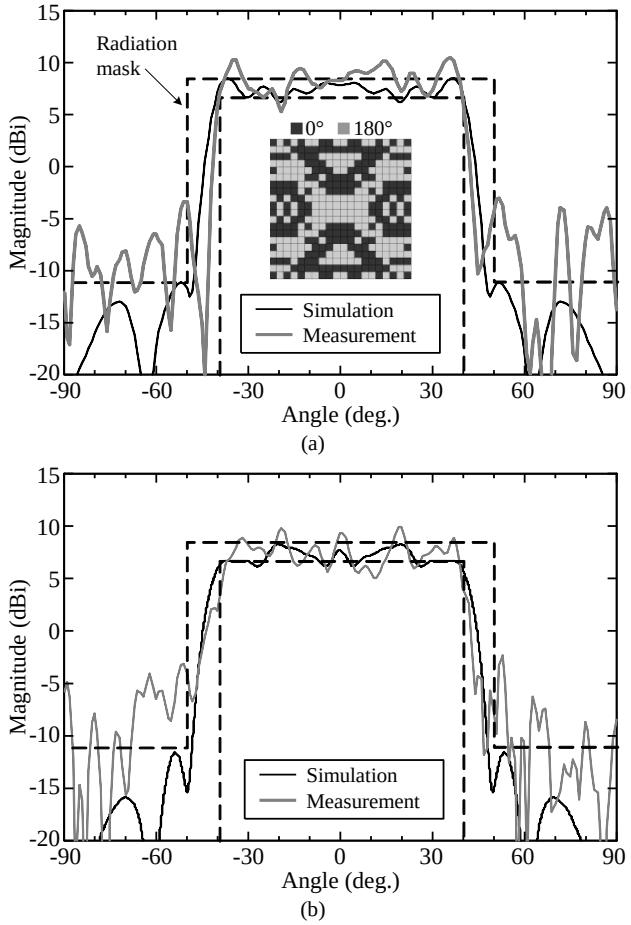

Fig. 15. Flat-top beam. Measured and simulated co-polarization components (a) H-plane and (b) E-plane (f = 9.8 GHz. F/D = 0.71).

The optimized antenna layout is represented in the inset of Fig. 15a, and the co-polarization components measured and computed in H- and E-planes are plotted in Figs. 15a and 15b, respectively. Although the ripple and side lobe levels are very slightly higher than the specified values, a satisfactory agreement is obtained between experiments and simulations.

The measured half-power beamwidth equals 82.6°. As these measurements have been performed in a 3 m-long anechoic chamber, the far-field conditions are not met, and this may explain part of the discrepancies observed between measurements and simulations, mainly in terms of ripple level (±2.2 dB) in the main beam. The SLL is equal to 12.2 dB and 13.5 dB in E- and H-planes, respectively. These values, higher than in simulations, can be explained by the spill-over radiation from the focal source and the diffraction along the array edges which are not taken into account in the numerical modeling.

IV. Conclusion

A 20×20-element linearly-polarized fully electronically-reconfigurable transmitarray is demonstrated in *X* band with excellent radiation performance (22.7 dBi maximum gain, 15.8% fractional 3-dB bandwidth, 52.9% peak efficiency). The array integrates 800 p-i-n diodes controlling the phase states of the array elements automatically and individually. The total DC power consumption is only 4.8 W. The multilayer stack-up, unit-cell topology and phase resolution (2 phase states, 1 bit) have been selected to find a good trade-off between complexity of the antenna architecture and radiation performance. The experimental results show excellent beam scanning characteristics in 2D over a 140°×80° angular sector. Satisfactory beam shaping characteristics have been demonstrated as well (flat-top beam).

Acknowledgment

This work has been partly funded by the Direction Générale de l'Armement (DGA/DS/MRIS), France. The authors would like to acknowledge the assistance of Philippe Klein (CEA) in the design of the steering logic boards, Alain Menard (DGA-MI) for radiation pattern measurements, and Anthony Rolland (IETR) for the synthesis of the flat top beam.

References

[1] J. Huang and J. A. Encinar, "Reflectarray antennas," *John Wiley & Sons Inc.*, Hoboken, NJ, 2007.

[2] B. Khayatian, Y. Rahmat-Samii, and J. Huang, "Radiation characteristics of reflectarray antennas: methodology and applications to dual configurations," *1st European Conf. Antennas and Propag., EuCAP 2006*, Nice, France, Nov. 2006.

[3] S. Xu, Y. Rahmat-Samii, and W. A. Imbriale, "Subreflectarrays for reflector surface distortion compensation," *IEEE Trans. Antennas Propag.*, vol. 57, no. 2, pp. 364–372, Feb. 2009.

[4] M. Arrebola, L. De Haro, J. A. Encinar, and L. F. De La Fuente, "Contoured-beam Gregorian antenna with a reflectarray as subreflector," *2nd European Conf. Antennas and Propag., EuCAP 2007*, Edinburgh, UK, Nov. 2007.

[5] M. Arrebola, L. de Haro, and J. A. Encinar, "Analysis of dual reflector antennas with a reflectarray as subreflector," *IEEE Antennas Propag. Mag.*, vol. 50, no. 6, pp. 39–51, Jun. 2008.

[6] W. Hu, M. Arrebola, R. Cahill, J. A. Encinar, V. Fusco, H. S. Gamble, Y. Alvarez, and F. Las-Heras, "94 GHz dual-reflector antenna with reflectarray subreflector," *IEEE Trans. Antennas Propag.*, vol. 57, no. 10, pp. 3043–3050, Oct. 2009.

[7] A. Clemente, L. Dussopt, R. Sauleau, P. Potier, and P. Pouliguen, "Multiple feed transmitarray antennas with reduced focal distance," *European Microwave Week, EuMW 2012*, Amsterdam, The Netherlands, 28 Oct.-2 Nov. 2012.

[8] H. Kaouach, L. Dussopt, J. Lantéri, R. Sauleau, and Th. Koleck, "Wideband low-loss linear and circular polarization transmitarray in V-band," *IEEE Trans. Antennas Propag.*, vol. 59, no. 7, pp. 2513–2523, Jul. 2011.

[9] A. Clemente, L. Dussopt, R. Sauleau, P. Potier, and P. Pouliguen, "Design and characterization of 2-bit passive unit-cells and transmitarrays in X-band," *5th European Conf. Antennas and Propag, EuCAP 2011*, Rome, Italy, 11-15 Apr. 2011.

[10] P. Padilla and M. Sierra-Castañer, "Design and prototype of a 12-GHz transmitarray," *Microw. Optical Tech. Lett.*, vol. 49, no. 12, pp. 3020–3026, Dec. 2007.

[11] P. Padilla and M. Sierra-Castañer, "Transmitarray for Ku band," *IEEE Antennas Propag. Soc. Int. Symp., AP-S/URSI 2007*, Honolulu (HA), Jun. 2007.

[12] R. H. Phillion and M. Okoniewski, "Lenses for circular polarization using planar arrays of rotated passive elements," *IEEE Trans. Antennas Propag.*, vol. 59, no. 4, pp. 1217–1227, Apr. 2011.

[13] P. Padilla de la Torre, A. Muñoz-Acevedo, M. Sierra-Castañer, and M. Sierra-Pérez, "Electronically reconfigurable transmitarray at Ku-band for microwave applications," *IEEE Trans. Antennas Propag.*, vol. 58, no. 8, pp.2571–2579, Aug. 2010.

[14] J. Y. Lau and S. V. Hum, "A planar reconfigurable aperture with lens and reflectarray modes operation," *IEEE Trans. Antennas Propag.*, vol. 58, no. 12, pp. 3547–3555, Dec. 2010.

[15] A. Clemente, L. Dussopt, B. Reig, R. Sauleau, P. Potier, and P. Pouliguen, "1-bit MEMS-based reconfigurable unit-cell for transmitarray antennas at X-band frequencies," *13th Int. Symp. RF*

MEMS and RF Micros., MEMSWAVE 2012, Antalya, Turkey, 2-4 Jul. 2012.

[16] C.-C. Cheng, B. Lakshminarayanan, and A. Abbaspour-Tamijani, "A programmable lens-array antenna with monolithically integrated MEMS switches," *IEEE Trans. Microwaves Theory Tech.*, vol. 57, no. 8, pp. 1874–1884, Aug. 2009.

[17] J. Y. Lau and S. V. Hum, "A wideband reconfigurable transmitarray element," *IEEE Trans. Antennas Propag*, vol. 60, no. 3, pp. 1303–1311, Mar. 2012.

[18] J. Y. Lau and S. V. Hum, "Reconfigurable transmitarray design approaches for beamforming applications," *IEEE Trans. Antennas Propag*, vol. 60, no. 12, pp. 5679–5689, Dec. 2012.

[19] L. Boccia, I. Russo, G. Amendola, and G. Di Massa , "Multilayer antenna-filter antenna for beam-steering transmitarray applications," *IEEE Trans. Microw. Theory Techn.*, vol. 60, no. 7, pp. 2287–2300, Jul. 2012.

[20] M. Sazegar, Y. Zheng, C. Kohler, H. Maune, M. Nikfalazar, J.R. Binder, R. Jakoby, "Beam steering transmitarray using tunable frequency selective sourface with integrated ferrolelectric varactors," *IEEE Trans. Antennas Propag.*, vol. 60, no. 12, pp. 5690-5699, Dec. 2012.

[21] A. Clemente, L. Dussopt, R. Sauleau, P. Potier, and P. Pouliguen, "1-bit reconfigurable unit-cell based on PIN diodes for transmitarray application in X-band," *IEEE Trans. Antennas Propag.*, vol. 60, no. 5, pp. 2260–2269, May 2012.

[22] A. Clemente, L. Dussopt, R. Sauleau, P. Potier, and P. Pouliguen, "Design of a reconfigurable transmitarray at X-band frequencies," *15th International Symp. Antenna Techn. Applied Electromagn., ANTEM 2012*, Toulouse, France, 25-28 Jun. 2012.

[23] E. Carrasco, M. Barba, and J. A. Encinar, "Electronically switchable-beam reflectarray antenna," *4th European Conf. Antennas Propag, EuCAP 2010*, Barcelona, Spain, Mar. 2010.

[24] C. Cheymol, T. Dousset, P. Dumon, M. Labeyrie, and C. Renard, "A X-band electronically scanned reflectarray antenna for space telemetry," *3rd European Conf. Antennas Propag, EuCAP 2009*, Berlin, Germany, Mar. 2009.

[25] J. Perruisseau-Carrier and A. K. Skrivervik, "Monolithic MEMS-based reflectarray cell digitally reconfigurable over a 360 degree phase range," *IEEE Antennas Wireless Propag. Lett.*, vol. 56, pp. 138–141, 2008.

[26] J. Perruisseau-Carrier, "Dual-polarized and polarization-flexible reflective cells with dynamic phase control," *IEEE Trans. Antennas Propag.*, vol. 58, no. 5, pp. 1494–1502, May 2010.

[27] R. Pereira, R. Gillard, R. Sauleau, P. Potier, T. Dousset, X. Delestre, "Dual linearly-polarized unit-cells with nearly 2-bit resolution for reflectarray applications in X-band," *IEEE Trans. Antennas Propag.*, vol. 60, no. 12, pp. 6042–6048, Dec. 2012.

[28] MA-COM Technology Solutions, MA4AGP907 and MA4AGFCP910 AlGaAs Flip Chip PIN Diodes [Online]. Available: www.macomtech.com/datasheets/MA4AGP907_FCP910.pdf.

[29] A. Trastoy, F. Ares, and E. Moreno, "Phase-only control of antenna sum and shaped patterns through null perturbation," *IEEE Antennas Propag. Mag.*, pp. 45–54, Dec. 2001.

[30] G. M. Kautz, "Phase-only shaped beam synthesis via technique of approximated beam addition," *IEEE Trans. Antennas Propag.*, vol. 47, no. 5, pp. 887–894, May 1999.

[31] O. M. Bucci, G. Franceschetti, G. Mazzarella, and G. Panariello, "Intersection approach to array pattern synthesis," *IEE Proc.*, vol. 137, pt. H, no. 6, pp. 349–357, Dec. 1990.

[32] S. Costanzo, F. Venneri, G. Di Massa, and G. Angiulli, "Synthesis of microstrip reflectarrays as planar scatters for SAR interferometry," *Elec. Lett.*, vol. 39, no. 3, pp. 266–267, Feb. 2003.

[33] J. A. Zornoza and J. A. Encinar, "Efficient phase-only synthesis of contoured-beam patterns for very large reflectarray," *Inter. Jour. RF and Microw. Computer-Aided Engin.*, vol. 14, pp. 415–423, Sep. 2004.

[34] B. Wu, A. Suntijo, M. E. Potter, and M. Okoniewski, "On the selection of the number of bits to control a dynamic MEMS reflectarray," *IEEE Antenna Wireless Propag. Letters*, vol. 7, pp. 183–186, 2008.

[35] S. Montori, C. Fritzsch, L. Marcaccioli, R. V. Gatti, R. Jakoby, and R. Sorrentino, "Design and measurement of a 1-bit reconfigurable elementary cell for large electronic steerable reflectarrays," *40th European Microwave Conference, EuMC 2010*, Paris, France, 28-30 Sep., 2010.

[36] H. Kamoda, T. Iwasaki, J. Tsumochi, T. Kuku, and O. Hashimoto, "60-GHz electrically reconfigurable large reflectarray using single-bit phase shifter," *IEEE Trans. Antennas Propag.*, vol. 59, no. 7, pp. 2524–2531, Jul. 2011.

[37] J. E. Roy and L. Shafai, "Generalization of the Ludwig-3 definition for linear copolarization and cross polarization," *IEEE Trans. Antennas Propag.*, vol. 49, no. 6, pp. 1006–1010, Jun. 2001.

[38] J. E. Roy and L. Shafai, "Corrections to "Generalization of the Ludwig-3 Definition for Linear Copolarization and Cross Polarization," *IEEE Trans. Antennas Propag.*, vol. 52, no. 2, pp. 638–639, Feb. 2004

[39] A. Rolland, M. Ettorre, M. Drissi, L Le Coq, and R. Sauleau, "Optimization of reduced-size smooth-walled conical horns using BoR-FDTD and genetic algorithm," *IEEE Trans. Antennas Propag.*, vol. 58, no. 9, pp. 3094–3100, Sep. 2010.

[40] A. Rolland, R. Sauleau, and L. Le Coq, "Flat shaped dielectric lens antenna for 60-GHz applications," *IEEE Trans. Antennas Propag.*, vol. 59, no. 11, pp. 4041–4048, Sep. 2011.

[41] G. Godi, R. Sauleau, L. Le Coq, and D. Thouroude, "Design and optimization of three dimensional integrated lens antennas with genetic algorithm," *IEEE Trans. Antennas Propag.*, vol. 55, no. 3, pp. 770–775, Mar. 2007.

Antonio Clemente received the B.S. and M.S. degree in telecommunication engineering and remote sensing systems from the University of Siena, Italy, in 2006 and 2009, and the Ph.D. degree in signal processing and telecommunications from the University of Rennes 1, France, in 2012. From October 2008 to May 2009 he realized his master thesis project at Technical University of Denmark (DTU), Lyngby, Denmark, where he worked on spherical near-field antenna measurements. His Ph.D. has been realized at CEA-LETI, Grenoble, France. In 2012, he joined the R&D laboratory of Satimo Industries, Villebon-sur-Yvette, France. Since 2013, he is a Research Engineer at CEA-LETI, Grenoble, France. His research interests include quasi-optic reconfigurable antennas at microwave and millimeter-wave frequencies, miniature integrated antennas, near-field and far-field antenna measurements.

Dr. Clemente received the Young Scientist Awards (First Prize) during the 15th International Symposium of Antenna Technology and Applied Electromagnetics 2012 (ANTEM 2012) in Toulouse, France.

Laurent Dussopt (S'00–A'01–M'03–SM'07) received the M.S. and Agrégation degrees in electrical engineering from the Ecole Normale Supérieure de Cachan, France, in 1994 and 1995, the Ph.D. degree in electrical engineering from the University of Nice-Sophia Antipolis, France, in 2000, and the "Habilitation à Diriger des Recherches" degree from the University Joseph Fourier, Grenoble, France, in 2008.

From September 2000 to October 2002, he was a Research Fellow with The University of Michigan at Ann Arbor. Since 2003, he is a Research Engineer at CEA-LETI, Grenoble, France. His research interests include reconfigurable antennas, millimetre-wave integrated antennas and antenna arrays, RF-MEMS devices and systems.

Dr. Dussopt received the Lavoisier Postdoctoral Fellowship from the French government in 2000 and was a co-recipient of the 2002 Best Student Paper Award (Second Prize) presented at the IEEE Radio Frequency Integrated Circuit (RFIC) Conference.

Ronan Sauleau (M'04–SM'06) graduated in electrical engineering and radio communications from the Institut National des Sciences Appliquées, Rennes, France, in 1995. He received the Agrégation degree from the Ecole Normale Supérieure de Cachan, France, in 1996, and the Doctoral degree in signal processing and telecommunications and the "Habilitation à Diriger des Recherches" degree from the University of Rennes 1, France, in 1999 and 2005, respectively.

He was an Assistant Professor and Associate Professor at the University of Rennes 1, between September 2000 and November 2005, and between December 2005 and October 2009, respectively. He has been appointed as a full Professor in the same University since November 2009. His current research fields are numerical modeling (mainly FDTD), millimeter-wave printed and reconfigurable

(MEMS) antennas, substrate integrated waveguide antennas, lens-based focusing devices, periodic and non-periodic structures (electromagnetic bandgap materials, metamaterials, reflectarrays, and transmitarrays) and biological effects of millimeter waves. He has been involved in more than 30 research projects at the national and European levels and has co-supervised 16 post-doctoral fellows, 24 PhD students, and 40 master students.
He has received eight patents and is the author or coauthor of more than 135 journal papers and 285 publications in international conferences and workshops. He has shared the responsibility of the research activities on antennas at IETR in 2010 and 2011. He is now co-responsible for the research Department 'Antenna and Microwave Devices' at IETR and is deputy director of IETR. Prof. Sauleau received the 2004 ISAP Conference Young Researcher Scientist Fellowship (Japan) and the first Young Researcher Prize in Brittany, France, in 2001 for his research work on gain-enhanced Fabry-Perot antennas. In September 2007, he was elevated to Junior member of the "Institut Universitaire de France". He was awarded the Bronze medal by CNRS in 2008. He was the co-recipient of several international conference awards with some of his students (Int. Sch. of BioEM 2005, BEMS'2006, MRRS'2008, E-MRS'2011, BEMS'2011, IMS'2012, Antem'2012). His was a guest editor for the IEEE Antennas Propogat. Special Issue on "Antennas and Propagation at mm and sub mm waves", 2013.

Patrick Potier received his degree of Ph. D. in structure and property of the material from the University of Rennes, Rennes, France, in 1984.
From September 1984 in September 1987, he was engineer of research in Thomson CSF, Paris, France. Since September 1987, he is an Engineer of Center "Maîtrise de l'information" (Information superiority) de la "Direction Générale de l'armement" (General Armaments Directorate, the French procurement agency). He treats the aspects antennas and radiation, and ensures the follow-up of various studies and theses mainly on the topics broad band reflect or transmit arrays.

Philippe Pouliguen was born in Rennes, France, on 1963. He received the M.S. degree in signal processing and telecommunications and the Ph.D. degree from the University of Rennes 1, France, in 1986 and 1990 respectively.
In 1990, he joined the Direction Générale de l'Armement (DGA) at the Centre d'Electronique de l'Armement (CELAR), in Bruz, France, where he was a "DGA expert" in electromagnetic radiation and radar signatures analysis. He was also in charge of the EMC (Expertise and ElectoMagnetism Computation) laboratory of CELAR. Now, he is the head of acoustic and radio-electric waves domain at the office for advanced research and innovation of the strategy directorate, DGA, France. His research interests include electromagnetic scattering and diffraction, Radar Cross Section (RCS) measurement and modeling, asymptotic high frequency methods, radar signal processing and analysis, antenna scattering problems and Electronic Band Gap Materials.
In these fields, he has published more than 30 articles in refereed journals and more than 80 conference papers.